

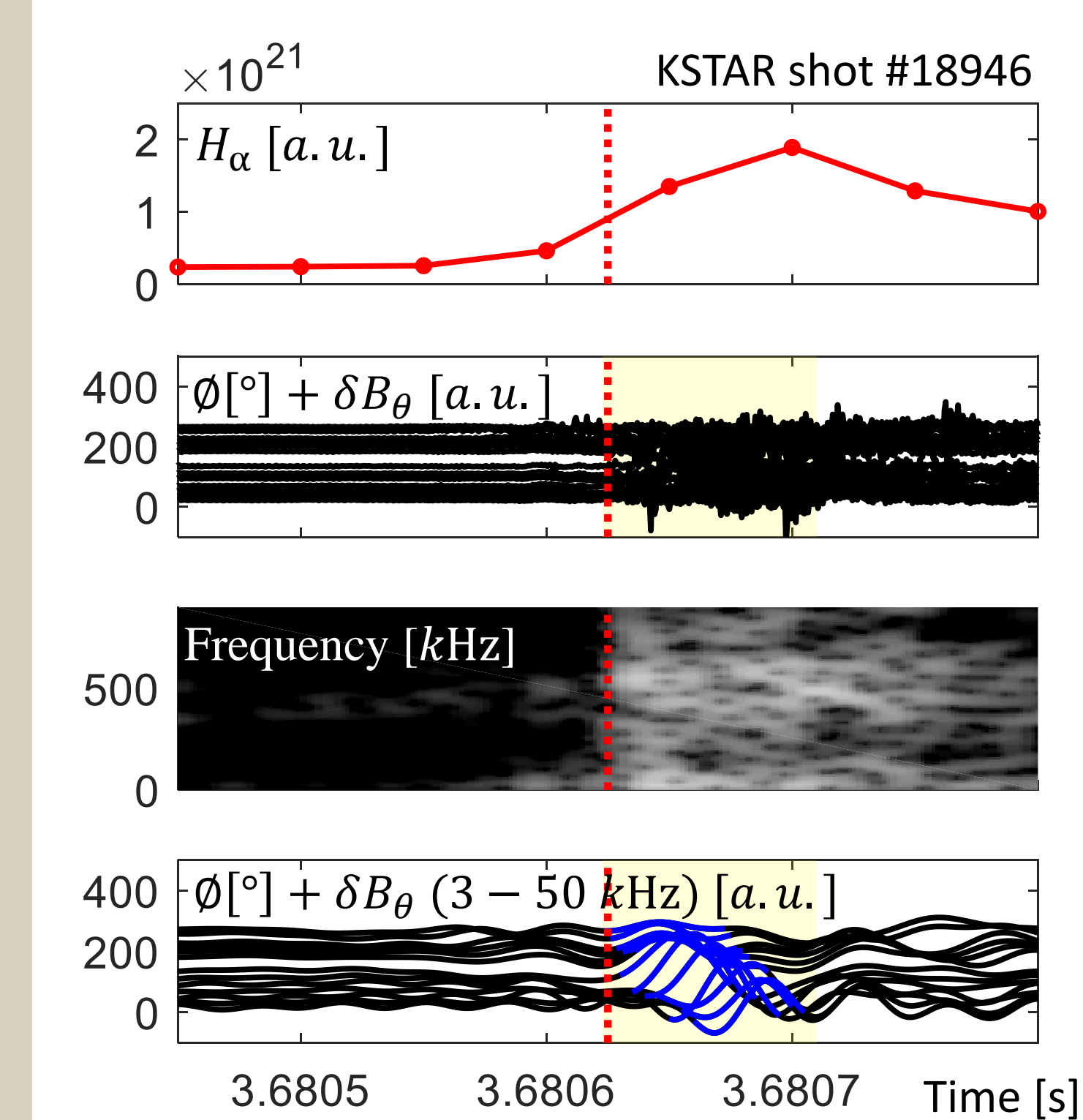
# Machine learning approach to understand the causality between solitary perturbation and edge confinement collapse in the KSTAR tokamak

J.E. Lee<sup>1</sup>, P. H. Seo<sup>1</sup>, J.G. Bak<sup>2,3</sup>, and G.S. Yun<sup>1</sup>  
<sup>1</sup>POSTECH, Korea <sup>2</sup>NFRI, Korea <sup>3</sup>KFE, Korea  
 jieun\_lee@postech.ac.kr

## Abstract

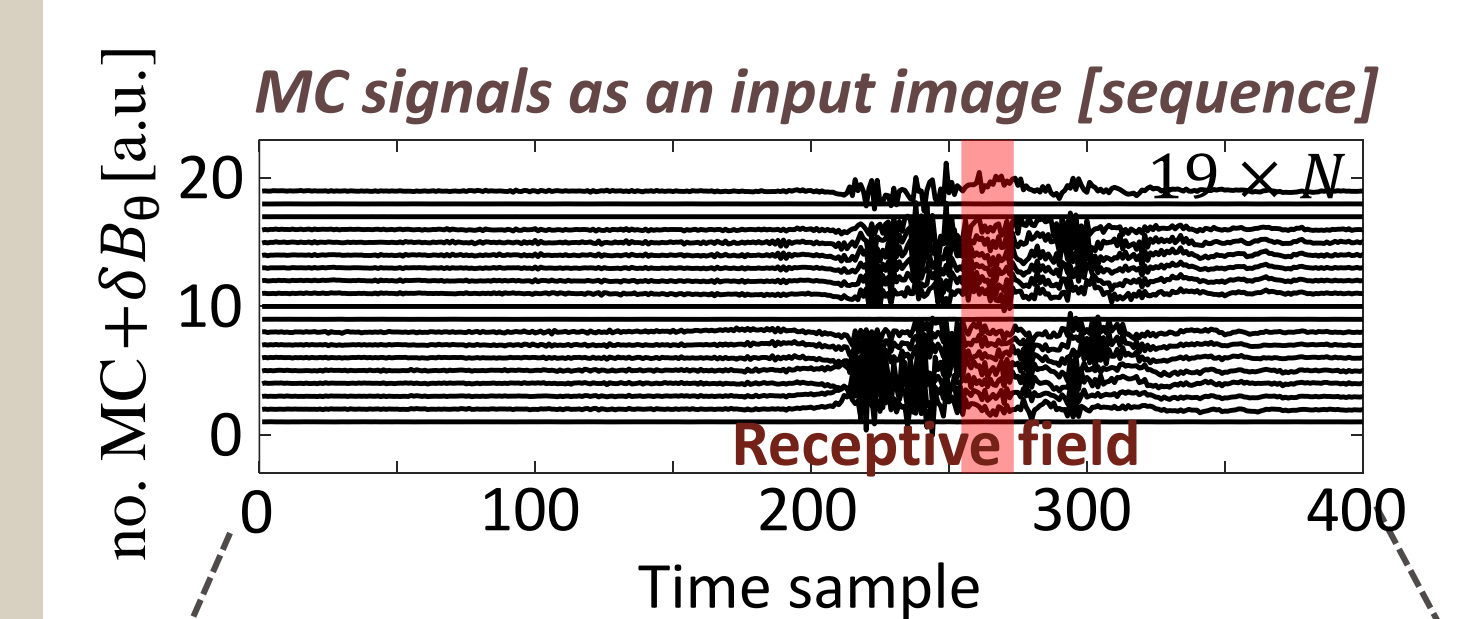
- Solitary perturbations (SPs) are detected within  $\sim 100 \mu\text{s}$  prior to the edge pedestal collapse in H-mode plasmas, which puts forward SP as a potential candidate for the edge pedestal collapse trigger.
- We have constructed an automatic SP identification model based on a convolutional deep neural network to enable a statistical study on the concurrency of SP and edge pedestal collapse.
- We applied the developed model to a large amount of data and confirmed that the complete collapse at the plasma boundary always involves the emergence of SP.

## Solitary Perturbation (SP)



- SP, localized in the poloidal direction, appear mostly tens of  $\mu\text{s}$  before the onset of the edge pedestal collapse.
- SP persists a few tens of  $\mu\text{s}$  to hundreds of  $\mu\text{s}$  without a noticeable change in shape.
- SP is clearly distinguished from ELM by spatial structure, amplitude, and flow velocity.

## Development of the SP identification model



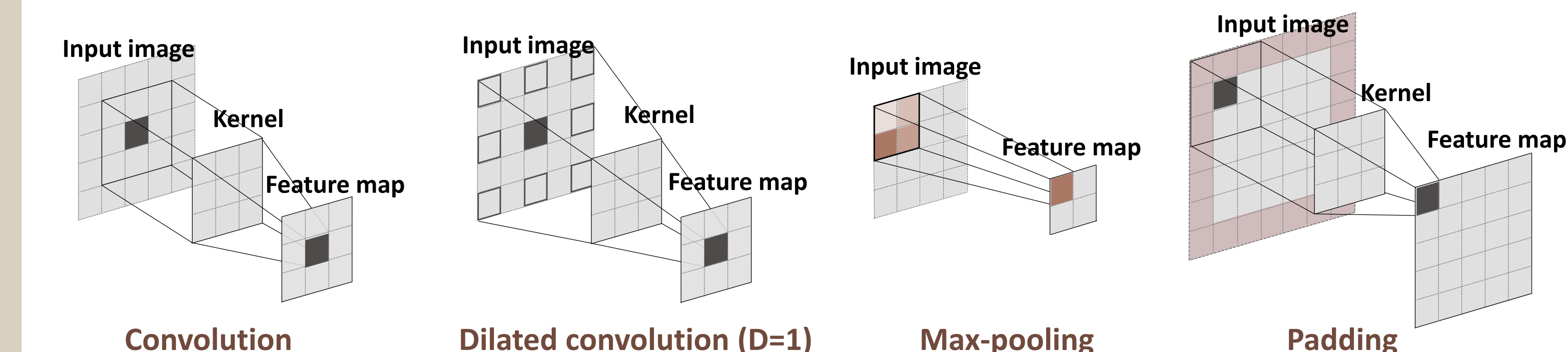
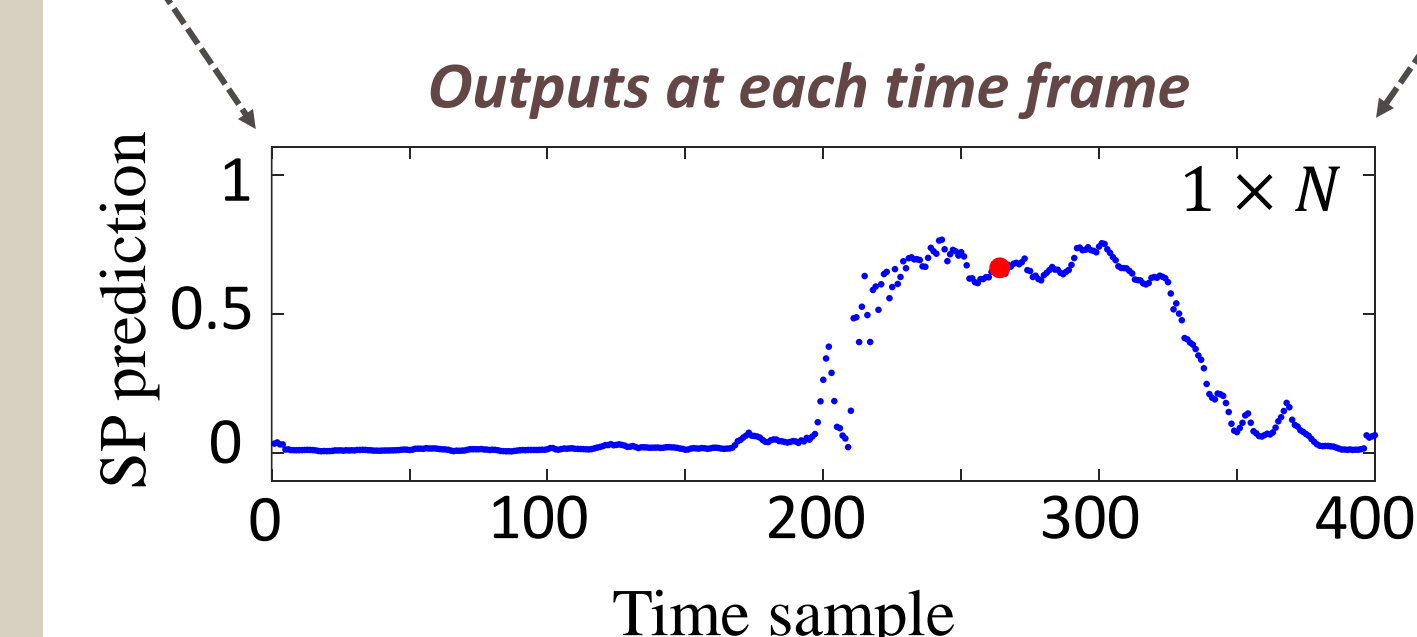
- **Input data**
  - Raw data of toroidal Mirnov coils
  - [no. MCs]  $\times$  [Time]:  $19 \times 400$
  - ; Toroidal array of MCs on KSTAR: 19
  - ; Time: 400 (400  $\mu\text{s}$ , 1 MHz sampling freq.)

- **Output data**
  - SP probability ( $0 \rightarrow 1$ )
  - [Time]: 400
  - ; Time: 400 (400  $\mu\text{s}$ , 1 MHz sampling freq.)

- **Network architecture**
  - 11 network layers
  - ; 7 Convolution + 3 Max-pooling + 1 Linear
  - Padding
  - ; Circular padding (coil dimension)
  - ; Zero padding (time dimension)

- **Training of the model**
  - Training dataset: 140 sequential data
  - ; 2015-2017 KSTAR discharges
  - ; 100 positive examples (w/ collapse and SP)
  - ; 20 negative examples (w/o collapse and SP)
  - ; 20 synthetic collapses examples (white noise  $\times$  envelope of MC signal)
  - Supervised learning
  - ; Minimization of errors between network output and correct answer

Layer		Output size
Operation	Dilation rate	
Convolution #1 (3 $\times$ 3@16)		19 $\times$ 400@16
Convolution #2 (3 $\times$ 1@16)		19 $\times$ 400@16
Convolution #3 (1 $\times$ 3@16)		19 $\times$ 400@16
Max-pooling #1 (1 $\times$ 2@16)		19 $\times$ 400@16
Convolution #4 (3 $\times$ 1@32)		19 $\times$ 400@32
Convolution #5 (1 $\times$ 3@32)	1	19 $\times$ 400@32
Maxpooling #2 (1 $\times$ 2@32)		19 $\times$ 400@32
Convolution #6 (3 $\times$ 1@32)		19 $\times$ 400@32
Convolution #7 (1 $\times$ 3@32)	3	19 $\times$ 400@32
Max-pooling #3 (19 $\times$ 1@32)		1 $\times$ 400@32
Linear (1 $\times$ 1@1)		1 $\times$ 400@1



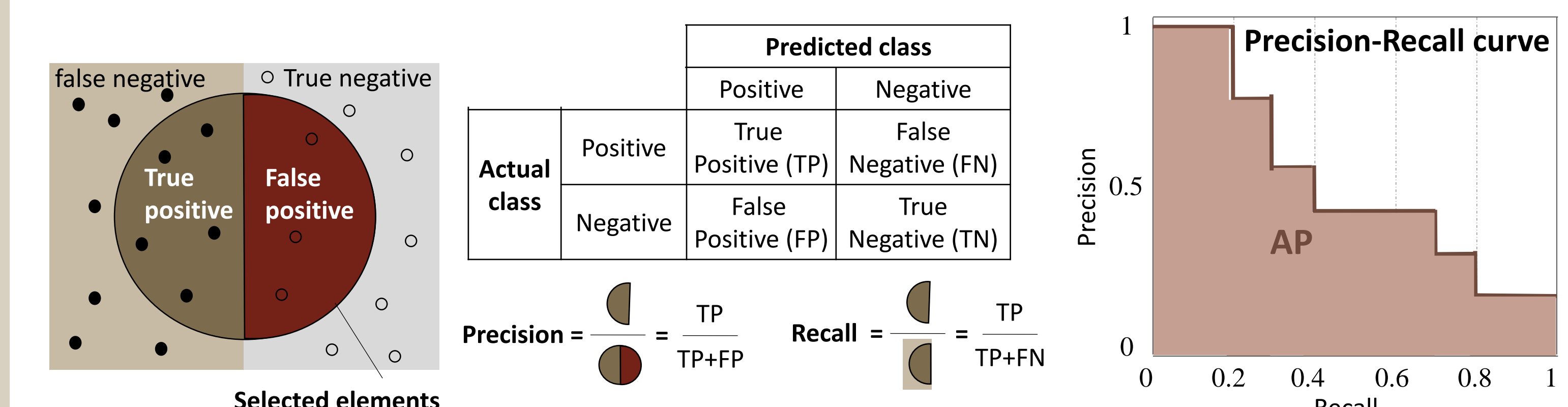
## Performance of the SP identification model

### Test of the model

- Test dataset: 50 sequential data (2015-2017 KSTAR discharges)
- ; 26 positive examples, 12 negative examples, 12 synthetic collapse examples

### Three metrics to evaluate the model

- **Per-frame accuracy (AF)**: The proportion of correct prediction of SP per frame
- **Per-sequence accuracy (AS)**: The proportion of correct prediction of SP per sequence
- **Average precision (AP)**: Mean precision over all possible threshold weighted by recall

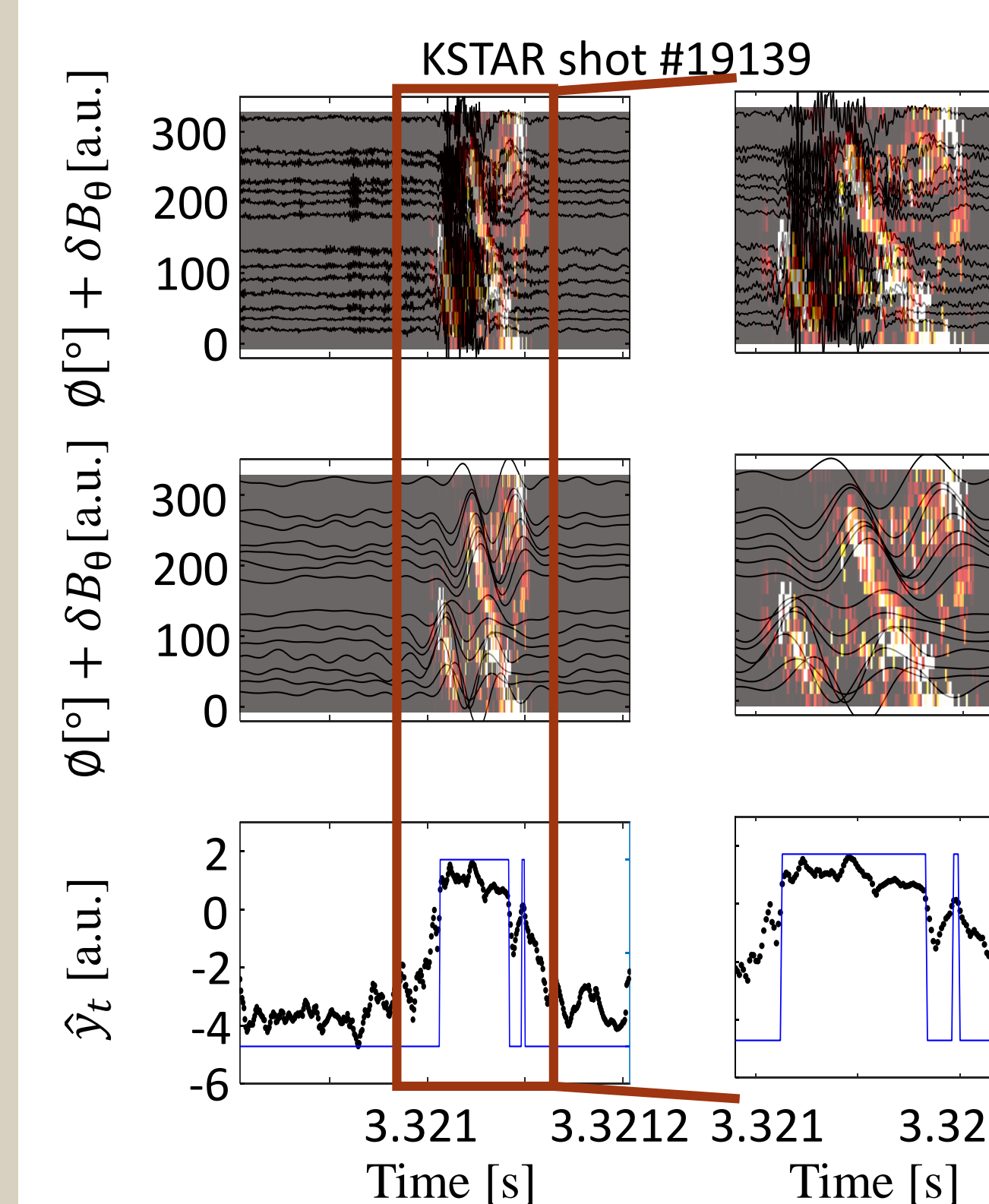


Metric	Result [%]
Accuracy	Time frame: 91.5
	Sequence: 100.0
Average Precision (AP)	88.5

### Quantitative performance of the model

- Threshold for the SP presence in time frame: 0.5
- Threshold for the SP presence in sequence ( $y_s$ ): 25
- AF for a trivial model which predicts a non-SP for every temporal frame is 82.5%.

## Qualitative validation by visualization



### Gradient based visualization technique

- Our Network is approximated by the 1<sup>st</sup> order Taylor expansion

$$\hat{y}_t \approx \mathbf{w}_t^T \mathbf{r} + b_t \quad \mathbf{w}_t = \frac{\partial \hat{y}_t}{\partial \mathbf{r}} \Big|_{\mathbf{r}_0}$$

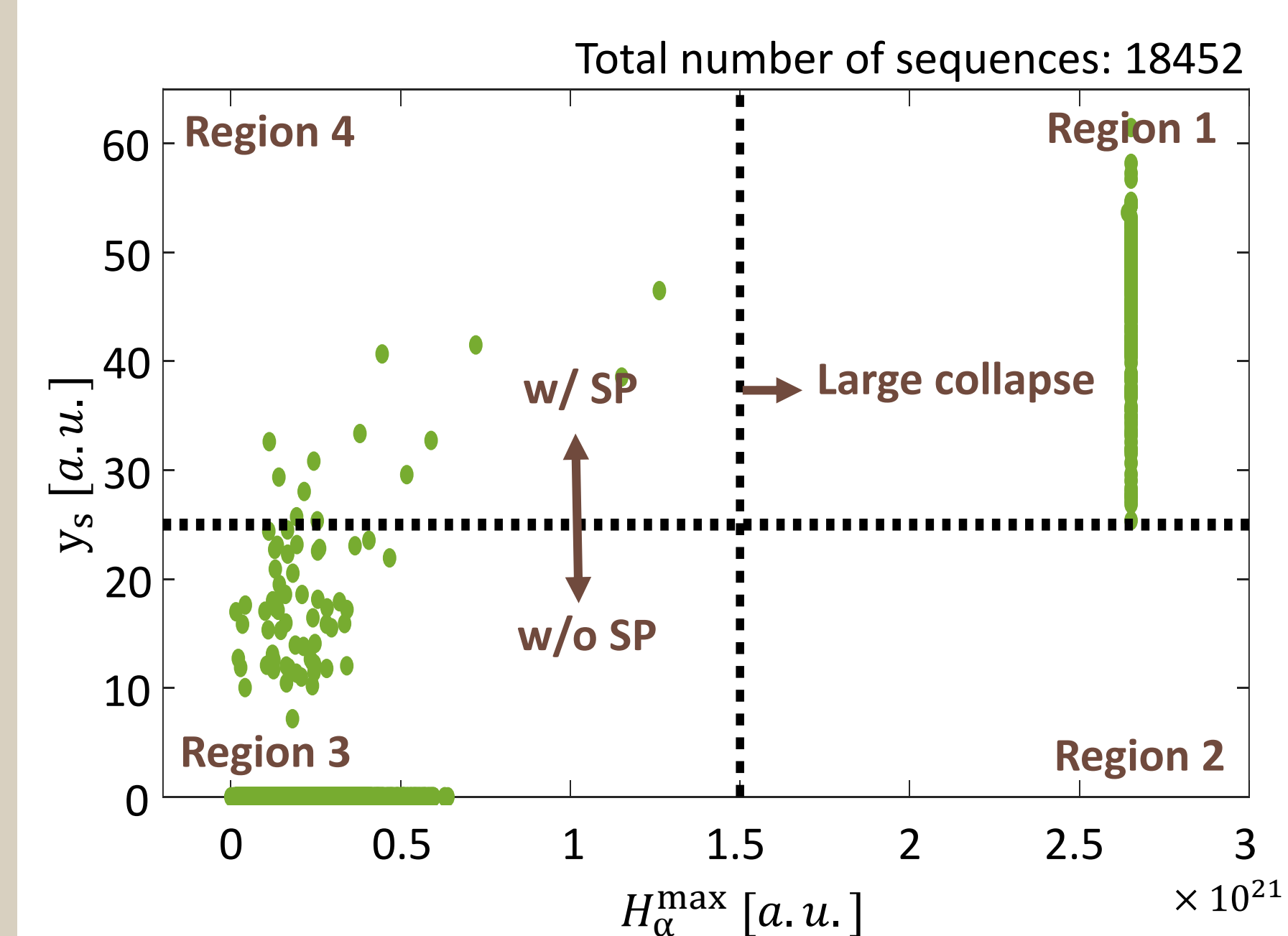
- ;  $\hat{y}_t$ : Input to the last sigmoid function ( $y_t = \text{sigmoid}(\hat{y}_t)$ )
- ;  $\mathbf{r}$ : Flattened vector of input  $X$ ,  $\in \mathbb{R}^{(19 \times N)}$
- ;  $\mathbf{w}_t$ : Gradient of  $\hat{y}_t$  at  $\mathbf{r}_0$ ,  $\in \mathbb{R}^{(19 \times N)}$

Heatmap by summing  $w_t$  at all positive frames

$$\mathbf{w}_H = \sum_{t \in P} \mathbf{w}_t = \frac{\partial}{\partial \mathbf{r}} \sum_{t \in P} \hat{y}_t \Big|_{\mathbf{r}_0}$$

The model predicts SPs by recognizing toroidally shifted SP patterns.

## Statistical analysis of the pedestal collapse-SP co-occurrence



### Statistical analysis data

- 2018 KSTAR discharges
- ; #20540, #20630, #20807, #21207

Region	Sequence #
1 (Large collapse w/ SP)	176
2 (Large collapse w/o SP)	0
3 (no large collapse w/o SP)	18263
4 (no large collapse w/ SP)	13

The complete edge pedestal collapse always involves the emergence of SP  
 → Studying the effect of SP on the edge pedestal collapse is essential for successful operation of fusion devices

## Acknowledgements

This work was supported by the NRF of Korea under grant No. NRF-2019M1A7A1A03088456. JL acknowledges the career development grant (No. WIST-2020-202) from the Center for WIST, funded by the MSIT. GY acknowledge the support by MSIT under IITP grant NO. 2019-0-01906.